Proposed Fluorination Mechanism of $CB_5H_6^-$ and $CB_9H_{10}^-$ with HF. Evidence of Kinetic Control in the Formation of 2-$CB_5H_5F^-$ and 6-$CB_9H_9F^-$

Michael L. McKee

Department of Chemistry, Auburn University, Auburn, Alabama 36849

Received February 9, 2001

Two pathways have been considered in the fluorination of $CB_5H_6^-$ and $CB_9H_{10}^-$ by HF. In the ionic HF fluorination pathway, the monocarborane anion cage is first protonated in a BBB face followed by H_2 elimination and fluoride anion addition. In the covalent HF fluorination pathway, HF is first coordinated through hydrogen to the BBB face. Next, the fluorine can add to either an axial or equatorial boron atom which opens the cage to a *nido* structure with an endo fluoride substituent. Endo to exo rearrangement occurs with a small activation barrier followed by H_2 elimination. In both pathways, fluorination at the equatorial boron position is predicted to have smaller activation barriers even though substitution at the axial position leads to the more stable products.

Introduction

In recent years there has been a surge of interest in weakly coordinating anions, especially carborane anions such as $CB_{11}H_{12}^-$.[1−8] The even distribution of negative charge in these cage systems allows these anions to be used as counteranions with a minimum of perturbation to the cationic system. For example, these anions have been used to form salts with SiR_3^+ and $C_{60}H^+$.[4k−n]

In the continuing effort to find even less-coordinating anions, cages have been synthesized with various substituents replacing hydrogen. Several methods have been used to add exosubstituents to the carborane cage. For example, it has been found that liquid anhydrous hydrogen fluoride (LAHF) provides a means to fluorinate positions in the hemisphere opposite to the carbon atom.[3]

It is of considerable interest that fluorination of the 12-vertex $CB_{11}H_{12}^-$ cage occurs first on the boron opposite carbon, while fluorination of $CB_9H_{10}^-$ does not produce any of the corresponding product.[3] The position opposite to carbon is known to be reactive. Heřmánek and co-workers[9] have investigated this effect, known as the antipodal effect, where there is increased reactivity of the antipodal B−H bond in heteroboranes with electrophiles and nucleophiles. Thus, consistent with this effect, LAHF fluorination of $CB_{11}H_{12}^-$ initially gives 12-$CB_{11}H_{11}F^-$, but under similar conditions, LAHF fluorination of $CB_9H_{10}^-$ initially gives 6-$CB_9H_9F^-$, not the expected 10-$CB_9H_9F^-$ product. With longer reaction times, the 7, 8, and 9 positions can also be fluorinated.

Computational Methods

All geometries were fully optimized in the given symmetry at the B3LYP/6-31G(d) level.[10] Vibrational frequencies, calculated at that level, determined the nature of the stationary points. Single-point energies at B3LYP/6-311+G(2d,p)//B3LYP/6-31G(d) with zero-point corrections at the B3LYP/6-31G(d) level constitute the "standard" level.

(1) (a) Reed, C. A. *Acc. Chem. Res.* **1998**, *31*, 133. (b) Reed, C. A. *Acc. Chem. Res.* **1998**, *31*, 325. (c) Strauss, S. H. *Chem. Rev.* **1993**, *93*, 927.

(2) (a) Ivanov, S. V.; Rockwell, J. J.; Polyakov, O. G.; Gaudinski, C. M.; Anderson, O. P.; Solntsev, K. A.; Strauss, S. H. *J. Am. Chem. Soc.* **1998**, *120*, 4224. (b) Ivanova, S. M.; Ivanov, S. V.; Miller, S. M.; Anderson, O. P.; Solntsev, K. A.; Strauss, S. H. *Inorg. Chem.* **1999**, *38*, 3756. (c) Lupinetti, A. J.; Havighurst, M. D.; Miller, S. M.; Anderson, O. P.; Strauss, S. H. *J. Am. Chem. Soc.* **1999**, *121*, 11920. (d) Ivanov, S. V.; Lupinetti, A. J.; Miller, S. M.; Anderson, O. P.; Solntsev, K. A.; Strauss, S. H. *Inorg. Chem.* **1995**, *34*, 6419. (e) Ivanov, S. V.; Lupinetti, A. J.; Solntsev, K. A.; Strauss, S. H. *J. Fluorine Chem.* **1998**, *89*, 65. (f) Ivanov, S. V.; Ivanova, S. M.; Miller, S. M.; Anderson, O. P.; Solntsev, K. A.; Strauss, S. H. *Inorg. Chim. Acta* **1999**, *289*, 76. (g) Ivanov, S. V.; Ivanova, S. M.; Miller, S. M.; Anderson, O. P.; Solntsev, K. A.; Strauss, S. H. *Inorg. Chem.* **1996**, *35*, 6914. (h) Ivanov, S. V.; Rockwell, J. J.; Lupinetti, A. J.; Solntsev, K. A.; Strauss, S. H. In *Advances in Boron Chemistry*; Siebert, W., Ed.; The Royal Chemical Society: Cambridge, 1997; p 430. (i) Strauss, S. H. In *Comtemporary Boron Chemistry*; Davidson, M., Hughes, A. K., Marder, T. B., Wade, K., Eds.; The Royal Chemical Society: Cambridge, 2000; p 44.

(3) Ivanov, S. V.; Rockwell, J. J.; Miller, S. M.; Anderson, O. P.; Solntsev, K. A.; Strauss, S. H. *Inorg. Chem.* **1996**, *35*, 7882.

(4) (a) Liston, D. J.; Lee, Y. J.; Scheidt, W. R.; Reed, C. A. *J. Am. Chem. Soc.* **1989**, *111*, 6643. (b) Jelínek, T.; Baldwin, P.; Scheidt, W. R.; Reed, C. A. *Inorg. Chem.* **1993**, *32*, 1982. (c) Xie, Z.; Jelínek, T.; Bau, R.; Reed, C. A. *J. Am. Chem. Soc.* **1994**, *116*, 1907. (d) Xie, Z.; Bau, R.; Reed, C. A. *Angew. Chem., Int. Ed. Engl.* **1994**, *33*, 2433. (e) Xie, Z.; Bau, R.; Reed, C. A. *Inorg. Chem.* **1995**, *34*, 5403. (f) Xie, Z.; Manning, J.; Reed, R. W.; Mathur, R.; Boyd, P. D. W.; Benesi, A.; Reed, C. A. *J. Am. Chem. Soc.* **1996**, *118*, 2922. (g) Bolskar, R. D.; Mathur, R. S.; Reed, C. A. *J. Am. Chem. Soc.* **1996**, *118*, 13093. (h) Reed, C. A.; Guiset, F. *J. Am. Chem. Soc.* **1996**, *118*, 3281. (i) Xie, Z.; Wu, B.-M.; Mak, T. C. W.; Manning, J.; Reed, C. A. *J. Chem. Soc., Dalton Trans.* **1997**, 1213. (j) Reed, C. A.; Fackler, N. L. P.; Kim, K.-C.; Stasko, D.; Evans, D. R. *J. Am. Chem. Soc.* **1999**, *121*, 6314. (k) RSi_3^+: Xie, Z.; Liston, D. L.; Jelínek, T.; Mitro, V.; Bau, R.; Reed, C. A. *J. Chem. Soc., Chem. Commun.* **1993**, 384. (l) RSi_3^+: Reed, C. A.; Xie, Z.; Bau, R.; Benesi, A. *Science* **1993**, *262*, 402. (m) RSi_3^+: Xie, Z.; Bau, R.; Benesi, A.; Reed, C. A. *Organometallics* **1995**, *14*, 3933. (n) HC_{60}^+: Reed, C. A.; Kim, K.-C.; Bolskar, R. D.; Mueller, L. J. *Science*, **2000**, *289*, 101.

(5) (a) Xie, Z.; Liu, Z.; Zhou, Z.-Y.; Mak, T. C. W. *J. Chem. Soc., Dalton Trans.* **1998**, 3367. (b) Evans, D. R.; Fackler, N. L. P.; Xie, Z.; Rickard, C. E. F.; Boyd, P. D. W.; Reed, C. A. *J. Am. Chem. Soc.* **1999**, *121*, 8466. (c) Tsang, C.-W.; Xie, Z. *Chem. Commun.* **2000**, 1839. (d) Tsang, C.-W.; Yang, Q.; Sze, E. T.-P.; Mak, T. C. W.; Chan, D. T. W.; Xie, Z. *Inorg. Chem.* **2000**, *39*, 5851. (e) Xie, Z.; Tsang, C.-W.; Xue, F.; Mak, T. C. W. *Inorg. Chem.* **1997**, *36*, 2246. (f) Xie, Z.; Tsang, C.-W.; Sze, E. T.-P.; Yang, Q.; Chan, D. T. W.; Mak, T. C. W. *Inorg. Chem.* **1998**, *37*, 6444. (g) Xie, Z.; Tsang, C.-W.; Xue, F.; Mak, T. C. W. J. *Organomet. Chem.* **1999**, *577*, 197. (h) Tsang, C.-W.; Yang, Q.; Sze, E. T.-P.; Mak, T. C. W.; Chan, D. T. W.; Xie, Z. *Inorg. Chem.* **2000**, *39*, 3582.

(6) Srivastava, R. R.; Hamlin, D. K.; Wilbur, D. S. *J. Org. Chem.* **1996**, *61*, 9041.

(7) King, B. T.; Janoušek, Z.; Grüner, B.; Trammel, M.; Noll, B. C.; Michl, J. *J. Am. Chem. Soc.* **1996**, *118*, 3313.

(8) Nestor, K.; Štíbr, B.; Kennedy, J. D.; Thornton-Pett, M.; Jelínek, T. *Collect. Czech. Chem. Commun.* **1992**, *57*, 1262.

(9) Heřmánek, S. *Inorg. Chim. Acta* **1999**, *289*, 20−44.

10.1021/ic010176h CCC: $20.00
Published on Web 09/28/2001

Table 1. Total Energies (hartrees) and Relative Energies (kcal/mol) for Species on the $CB_5H_6^-$/HF and $CB_9H_{10}^-$/HF Potential Energy Surface[a]

					rel energies (kcal/mol)			
					B3LYP/6-31G(d)		B3LYP/6-311+G(2d,p)	
	pg[b]	B3LYP/6-31G(d)	ZPE (NIF)	B3LYP/6-311+G(2d,p)	*E*	*E* + ZPC	*E*	*E* + ZPC
H_2	$D_{\infty h}$	−1.17548	6.36(0)	−1.17957				
HF	$C_{\infty v}$	−100.42017	5.69(0)	−100.48306	0.0	0.0	0.0	0.0
F^-	*K*	−99.75409	0.00(0)	−99.88869	418.0	412.3	373.0	367.3
$(HF)_2$	C_{2h}	−200.85563	13.63(0)	−200.97078	0.0	0.0	0.0	0.0
FHF^-	$D_{\infty h}$	−200.28346	6.50(0)	−200.44705	359.0	351.9	328.6	321.5
A1−H^+ (CB_5H_7)	C_s	−166.56950	58.10(0)	−166.61327	0.0	0.0	0.0	0.0
A1	C_{4v}	−166.05271	51.43(0)	−166.10680	324.3	317.6	317.8	311.1
CB_5H_5(ax)·H_2 (TS)	C_s	−166.51668	54.77(1)	−166.56478	33.1	30.8	30.4	28.1
CB_5H_5(ax)·H_2	C_{2v}	−166.51791	56.29(0)	−166.56768	32.4	31.5	28.6	27.8
CB_5H_5(ax)	C_{4v}	−165.30637	44.93(0)	−165.34778				
CB_5H_5(ax) + H_2		−166.48185	51.29	−166.52735	55.0	49.2	53.9	48.1
CB_5H_5(eq)	C_s	−165.29886	44.60(0)	−165.33992				
CB_5H_5(eq) + H_2		−166.47434	50.96	−166.51949	59.7	53.6	58.8	52.7
B1−H^+ (CB_9H_{11})	C_s	−268.46815	94.94(0)	−268.52883	0.0	0.0	0.0	0.0
B1	C_{4v}	−267.99916	88.98(0)	−268.06600	294.3	288.3	290.4	284.5
CB_9H_9(ax)·H_2	C_{2v}	−268.44822	94.19(0)	−268.51422	12.5	12.0	9.2	8.7
CB_9H_9(eq)·H_2 (TS)	C_s	−268.44026	93.94(1)	−268.50645	17.5	16.8	14.0	13.3
CB_9H_9(ax)	C_{4v}	−267.23671	82.63(0)	−267.29390				
CB_9H_9(ax) + H_2		−268.41219	88.99	−268.47347	35.1	29.4	34.7	29.1
CB_9H_9(eq)	C_s	−267.25173	82.74(0)	−267.30874				
CB_9H_9(eq) + H_2		−268.42721	89.10	−268.48831	25.7	20.1	25.4	19.9
A1+HF		−266.47288	57.12	−266.58986	0.0	0.0	0.0	0.0
A1−H^++F^-		−266.32359	58.10	−266.50196	93.7	94.7	55.2	56.1
A2·HF	C_s	−266.49794	58.98(0)	−266.60998	−15.7	−13.9	−12.6	−10.8
TSA2/A3	C_s	−266.42417	56.49(1)	−266.53134	30.6	29.9	36.7	36.1
TSA2/A6	C_1	−266.42564	56.14(1)	−266.53199	29.6	28.7	36.3	35.3
A3	C_s	−266.48777	58.90(0)	−266.58419	−9.3	−7.6	3.6	5.3
TSA3/A4	C_1	−266.45586	57.78(1)	−266.55469	10.7	11.3	22.1	22.7
A4	C_s	−266.49615	59.35(0)	−266.59347	−14.6	−12.4	−2.3	0.0
TSA4/A5+H_2	C_s	−266.40785	55.00(1)	−266.51188	40.8	38.7	48.9	46.8
A5	C_{4v}	−265.34900	47.76(0)	−265.44229				
A5+H_2		−266.52448	54.12	−266.62186	−32.4	−35.4	−20.1	−23.1
A6	C_1	−266.49704	59.11(0)	−266.59349	−15.2	−13.2	−2.3	−0.3
TSA6/A7	C_1	−266.46423	57.60(1)	−266.56302	5.4	5.9	16.8	17.3
[**TSA6/A7**]′	C_1	−266.46268	57.35(1)	−266.56069	6.4	6.6	18.3	18.5
A7	C_1	−266.50404	59.36(0)	−266.60162	−19.6	−17.3	−7.4	−5.1
TSA7/A8+H_2	C_1	−266.41122	55.03(1)	−266.51422	38.7	36.6	47.5	45.4
A8	C_s	−265.34721	47.64(0)	−265.44028				
A8+H_2		−266.52269	54.00	−266.61985	−31.3	−34.4	−18.8	−21.9
$CB_5H_7F^-$ (**A9**)	C_1	−266.53161	59.73(0)	−266.63021	−36.8	−34.2	−25.3	−22.7
B1+HF		−368.41933	94.67	−368.54906	0.0	0.0	0.0	0.0
B1−H^++F^-		−368.22224	94.94	−368.41752	123.7	123.9	82.5	82.8
B2	C_s	−368.43860	95.99(0)	−368.56360	−12.1	−10.8	−9.1	−7.8
TSB2/B3	C_s	−368.33122	92.69(1)	−368.44465	55.3	53.3	65.5	63.5
TSB2/B6	C_1	−368.34535	93.12(1)	−368.45939	46.4	44.9	56.3	54.7
B3	C_s	−368.38515	95.15(0)	−368.49611	21.4	21.9	33.2	33.7
TSB3/B4	C_s	−368.36768	93.58(1)	−368.48170	32.4	31.3	42.3	41.2
B4	C_s	−368.39252	95.79(0)	−368.50519	16.8	17.9	27.5	28.6
TSB4/B5+H_2	C_s	−368.33875	93.12(1)	−368.45635	50.6	49.0	58.2	56.6
[**TSB4/B5**+H_2]′	C_s	−368.33206	91.76(2)	−368.44983	54.8	51.8	62.3	59.4
B5	C_{4v}	−367.29295	85.10(0)	−367.39832				
B5+H_2		−368.46843	91.46	−368.57789	−30.8	−34.0	−18.1	−21.3
B6	C_1	−368.39610	95.95(0)	−368.50627	14.6	15.9	26.8	28.1
TSB6/B7	C_1	−368.36043	94.36(1)	−368.47274	37.0	36.6	47.9	47.6
[**TSB6/B7**]′	C_1	−368.35899	94.05(1)	−368.47137	37.9	37.2	48.8	48.1
B7	C_1	−368.41374	96.03(0)	−368.52564	3.5	4.9	14.7	16.1
TSB7/B8+H_2		−368.36080	93.80(1)	−368.47768	36.7	35.9	44.8	43.9
B8	C_s	−367.29104	84.89(0)	−367.39665				
B8+H_2		−368.46652	91.25	−368.57622	−29.6	−33.0	−17.0	−20.5
A1+2HF		−366.89305	62.81	−367.07292	0.0	0.0	0.0	0.0
A1+$(HF)_2$		−366.90834	65.06	−367.07758	−9.6	−7.3	−2.9	−0.7
A2·2HF	C_s	−366.94547	66.76(0)	−367.11332	−32.9	−28.9	−25.4	−21.4
TSA2·2HF/**A3**+HF	C_s	−366.89326	65.86(2)	−367.06038	−0.1	2.9	7.9	10.9
A3+HF		−366.90847	64.59	−367.06725	−9.7	−7.9	3.6	5.3
TSA2·2HF/**A6**+HF	C_1	−366.89338	65.42(2)	−367.06314	−0.2	2.4	6.1	8.7
A3+HF		−366.91721	64.80	−367.07655	−15.2	−13.2	−2.3	−0.3
TSA2·2HF/**A1**−H^++FHF^-	C_1	−366.90042	65.20(1)	−367.07216	−4.6	−2.2	0.5	2.9
A1−H^++FHF^-		−366.85296	64.60	−367.06031	25.2	26.9	7.9	9.7

[a] The symbols **A1** and **B1** represent the cages $CB_5H_6^-$ and $CB_9H_{10}^-$, respectively. [b] Point group.

The B3LYP/6-31G(d) geometries for boranes and carboranes have been shown to be accurate and comparable to those at MP2/6-31G(d).[11] Total energies (hartrees), zero-point energies (kcal/mol), and relative energies (kcal/mol) are given in Table 1. Cartesian coordinates of all species are provided as Supporting Information.

Results and Discussion

The boron hydride dianions ($B_nH_n^{2-}$) and monocarborane anions ($CB_nH_{n+1}^-$) all have *closo* electron counts and have been studied extensively due to their high stability and aromatic character.[12−16] In a series of papers, Schleyer and co-workers[16] have studied the protonation of the boron hydride dianion series. For the $B_6H_6^{2-}$, $B_{10}H_{10}^{2-}$, and $B_{12}H_{12}^{2-}$ cages, the most stable site of protonation is in the middle of a BBB triangular face (face-protonated). These systems are fluxional and have generally small barriers to edge-protonation and B-protonation. Protonation of a monocarborane anion ($CB_nH_{n+1}^-$) produces a neutral carborane (CB_nH_{n+2}). The only known member of this series is CB_5H_7, which is face-protonated.[17,18]

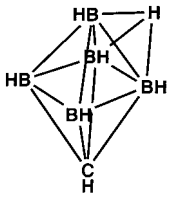

In Table 2, the calculated proton affinities are given for $B_nH_n^{2-}$ and $CB_nH_{n+1}^-$ for 6-, 10-, and 12-vertex cages. As the size of the cage increases for the boron hydride dianions and monocarborane anions, the proton affinity decreases. This trend is due to the larger number of atoms to accommodate the negative charge. In all systems studied to date, the most stable site of protonation in the monocarborane is in a BBB face in the hemisphere opposite to the carbon atom.

Some comment is necessary regarding the nature of the fluorinating agent. When liquid anhydrous hydrogen fluoride (LAHF) is used, the high dielectric constant ($\epsilon = 83.6$)[19] will provide a very polar evironment. In the gas phase, the proton affinity of F^- ($HF \rightarrow F^- + H^+$) is very large (371.8 kcal/mol).[20] However, the proton affinities of $(HF)_n{\cdot}F^-$ complexes are much smaller.[20] Calculations at the MP2/6-311++G(d,p) level for $H_{n-1}F_n^-$ ($(HF)_n \rightarrow H_{n-1}F_n^- + H^+$), $n = 1-5$ indicate that the proton affinity (PA) of F^- ($n = 1$) decreases from 371.8 kcal/mol to 322.8 (HF_2^-, $n = 2$), 287.5 ($H_2F_3^-$, $n = 3$), 255.9 ($H_3F_4^-$, $n = 4$), and 231.8 kcal/mol ($H_4F_5^-$, $n = 5$) (see Table 2).

The calculated PA values of $CB_5H_6^-$ (Figure 1, 311.1 kcal/mol) and $CB_9H_{10}^-$ (284.5 kcal/mol) suggest that the monocarboranes may be protonated in LAHF (eq 1).

$$CB_9H_{10}^- + (HF)_5 \rightarrow CB_9H_{11} + H_4F_5^- \qquad (1)$$

$$(\Delta H_{rxn} = -52.7 \text{ kcal/mol})$$

Table 2. Table of Proton Affinities (kcal/mol) of *closo*-Boron Hydride Dianions, *closo*-Monocarborane Anions, and $(HF)_n{\cdot}F^-$ Complexes[a,b]

PA	reaction	PA
$B_6H_6^{2-}$	$B_6H_7^- \rightarrow B_6H_6^{2-} + H^+$	431.9[c]
$B_{10}H_{10}^{2-}$	$B_{10}H_{11}^- \rightarrow B_{10}H_{10}^{2-} + H^+$	391.1[c]
$B_{12}H_{12}^{2-}$	$B_{12}H_{13}^- \rightarrow B_{12}H_{12}^{2-} + H^+$	366.1[c]
$CB_5H_6^-$	$CB_5H_7 \rightarrow CB_5H_6^- + H^+$	311.1[d]
$CB_9H_{10}^-$	$CB_9H_{11} \rightarrow CB_9H_{10}^- + H^+$	284.5[d]
$CB_{11}H_{12}^-$	$CB_{11}H_{13} \rightarrow CB_{11}H_{12}^- + H^+$	267.8[e] (264.8)[f]
F^-	$HF \rightarrow F^- + H^+$	367.3[d] (371.8)[g]
FHF^-	$(HF)_2 \rightarrow FHF^- + H^+$	321.5[d] (322.8)[g]
$H_2F_3^-$	$(HF)_3 \rightarrow H_2F_3^- + H^+$	(287.5)[g]
$H_3F_4^-$	$(HF)_4 \rightarrow H_3F_4^- + H^+$	(255.9)[g]
$H_4F_5^-$	$(HF)_5 \rightarrow H_4F_5^- + H^+$	(231.8)[g]

[a] The gas-phase acidity of AH_g is the free energy change of the reaction $AH \rightarrow A^- + H^+$, while the proton affinity of A^-_g is the enthalpy change for the same reaction. [b] All cages are face-protonated. In $CB_nH_{n+1}^-$ carborane anions, all cages are protonated in the hemisphere opposite to the carbon aton. In $CB_{11}H_{12}^-$, B-protonation on the 12-position is 3.0 kcal/mol more stable than face-protonation. [c] Enthalpy calculated at B3LYP/6-311+G(d,p)//B3LYP/6-31G(d) at 0 K; ref 16c. [d] This work. Enthalpy at B3LYP/6-311+G(2d,p)//B3LYP/6-31G(d) at 0 K. [e] 12-B protonated. Enthalpy calculated at B3LYP/6-31+G(d) at 298 K; ref 14. [f] 7-8-12-BBB face-protonated. Enthalpy calculated at B3LYP/6-31+G(d) at 298 K; ref 14. [g] Enthalpy calculated at MP2/6-311++G(d,p) at 298 K; ref 20.

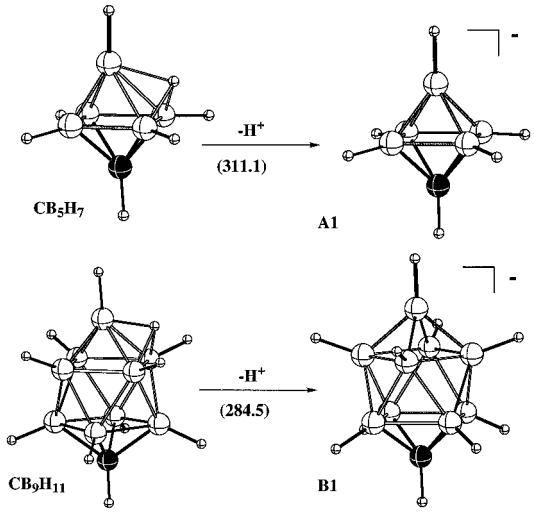

Figure 1. Molecular plots of CB_5H_7, $CB_5H_6^-$ (**A1**), CB_9H_{11}, and $CB_9H_{10}^-$ (**B1**). The proton affinities (B3LYP/6-311+G(2d,p)//B3LYP/6-31G(d)+ZPC) of $CB_5H_6^-$ and $CB_9H_{10}^-$ are 311.1 and 284.5 kcal/mol, respectively.

(10) Frisch, M. J.; Trucks, G. W.; Schlegel, H. B.; Scuseria, G. E.; Robb, M. A.; Cheeseman, J. R.; Zakrzewski, V. G.; Montgomery, J. A., Jr.; Stratmann, R. E.; Burant, J. C.; Dapprich, S.; Millam, J. M.; Daniels, A. D.; Kudin, K. N.; Strain, M. C.; Farkas, O.; Tomasi, J.; Barone, V.; Cossi, M.; Cammi, R.; Mennucci, B.; Pomelli, C.; Adamo, C.; Clifford, S.; Ochterski, J.; Petersson, G. A.; Ayala, P. Y.; Cui, Q.; Morokuma, K.; Malick, D. K.; Rabuck, A. D.; Raghavachari, K.; Foresman, J. B.; Cioslowski, J.; Ortiz, J. V.; Stefanov, B. B.; Liu, G.; Liashenko, A.; Piskorz, P.; Komaromi, I.; Gomperts, R.; Martin, R. L.; Fox, D. J.; Keith, T.; Al-Laham, M. A.; Peng, C. Y.; Nanayakkara, A.; Gonzalez, C.; Challacombe, M.; Gill, P. M. W.; Johnson, B.; Chen, W.; Wong, M. W.; Andres, J. L.; Gonzalez, C.; Head-Gordon, M.; Replogle, E. S.; Pople, J. A. *Gaussian 98*; Gaussian, Inc.: Pittsburgh, PA, 1998.

(11) See: (a) *The Encyclopedia of Computational Chemistry*; Schleyer, P. v. R., Allinger, N. L., Clark, T., Gasteiger, J., Kollman, P. A., Schaefer, H. F., III., Schreiner, P. R., Eds.; John Wiley & Sons: Chichester, 1998. (b) Koch, W.; Holthausen, M. C. *A Chemist's Guide to Density Functional Theory*; Wiley-VCH: Weinheim, 2000; pp 195−209.

(12) McKee, M. L. *J. Am. Chem. Soc.* **1997**, *119*, 4220.

(13) McLemore, D. K.; Dixon, D. A.; Strauss, S. H. *Inorg. Chim. Acta* **1999**, *294*, 193.

(14) Koppel, I. A.; Burk, P.; Koppel, I.; Leito, I.; Sonoda, T.; Mishima, M. *J. Am. Chem. Soc.* **2000**, *122*, 5114.

(15) Hermansson, K.; Wójcik, M.; Sjöberg, S. *Inorg. Chem.* **1999**, *38*, 6039.

(16) (a) McKee, M. L.; Bühl, M.; Charkin, Oleg P.; Schleyer, P. v. R. *Inorg. Chem.* **1993**, *32*, 4549. (b) Schleyer, P. v. R.; Najafian, K. *Inorg. Chem.* **1998**, *37*, 3454. (c) Mebel, A. M.; Schleyer, P. v. R.; Najafian, K.; Charkin, O. P. *Inorg. Chem.* **1998**, *37*, 1693. (d) Mebel, A. M.; Charkin, O. P.; Bühl, M.; Schleyer, P. v. R. *Inorg. Chem.* **1993**, *32*, 463.

(17) Grimes, R. N. *Carboranes*; Academic Press: New York, 1970.

(18) Štíbr, B. *Chem. Rev.* **1992**, *92*, 225.

Scheme 1

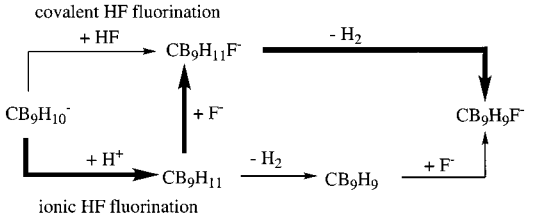

Two fluorination pathways are considered: covalent HF addition where the H−F bond remains intact; and ionic HF addition where H^+ adds first (Scheme 1).

McLemore et al.[13] calculated a series of 12-vertex fluorinated and unfluorinated monocarborane cages using density functional theory. From experiment, it is known that fluorination of $CB_{11}H_{12}^-$ with LAHF produces 12-$CB_{11}H_{11}F^-$ rather than 7-$CB_{11}H_{11}F^-$. From calculations, is was found that 7-$CB_{11}H_{11}F^-$ was 0.7 kcal/mol more stable than 12-$CB_{11}H_{11}F^-$ at the NLDFT+ZPC level,[14] which indicated that the fluorination was under kinetic control rather than thermodynamic control. They also calculated the 7-$CB_{11}H_{11}$ and 12-$CB_{11}H_{11}$ cages and found the latter to be 4.5 kcal/mol more stable than the former.[14]

Onak and co-workers[21] have reacted tetrabutylammonium fluoride with various *closo* carboranes in THF at room temperature and found that the fluoride ion opened a *closo* cage to a *nido* structure. In the fluorination of *closo*-1,6-$C_2B_4H_6$ under these conditions 5-F-*nido*-2,4-$C_2B_4H_6^-$ was formed (see below). The structure of the product was determined by using IGLO to determine the experimental NMR spectra.[22]

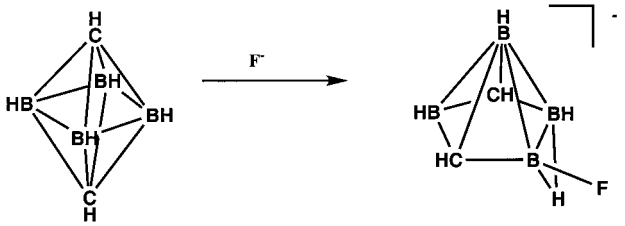

A computational study of fluorination by LAHF of $CB_5H_6^-$ and $CB_9H_{10}^-$ has been undertaken. While fluorination of $CB_5H_6^-$ has not been reported, the anion has a structure similar to $CB_9H_{10}^-$ (i.e., both anions have C_{4v} point group with the carbon atom on the 4-fold axis). Therefore, calculations on the simpler 6-vertex cage may serve as a model for mimina and transition states for the larger 10-vertex system.

Ionic HF Fluorination. After protonation of $CB_5H_6^-$, H_2 can be eliminated in a concerted fashion by taking the capping hydrogen and either the B−H(ax) hydrogen or one of the four B−H(eq) hydrogens. A transition state was located for the formation of a $CB_5H_5{\cdot}H_2$ complex which was 28.1 kcal/mol higher than CB_5H_7 (Figure 2). The H−H distance in the transition state is 1.095 Å, which was reduced to 0.901 Å in the complex. It was assumed that no transition state exists for elimination of H_2 from the complex, which means that the activation barrier for elimination of H_2 from CB_5H_7 is the endothermicity of the reaction $CB_5H_7 \rightarrow CB_5H_5(ax) + H_2$ (48.1 kcal/mol). Furthermore, it was assumed that the $CB_5H_5(ax)$ species will add fluoride (F^-) without barrier to form **A5**. When a capping and equatorial hydrogen are removed, an intermediate H_2 complex is not found and the assumed barrier is the endothermicity of the reaction $CB_5H_7 \rightarrow CB_5H_5(eq) + H_2$ to form **A8** (52.7 kcal/mol), which is 4.6 kcal/mol higher than the H_2 (capping-axial) pathway.

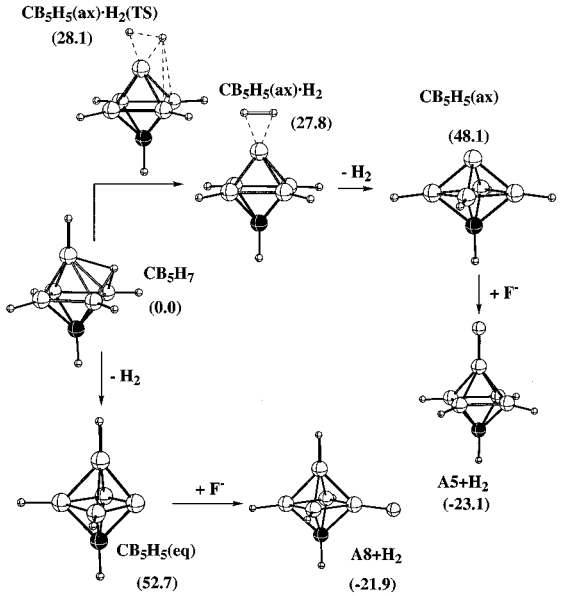

Figure 2. Ionic HF fluorination pathway of $CB_5H_6^-$. $CB_5H_5(ax)$ is 4.6 kcal/mol more stable than $CB_5H_5(eq)$. All energies (kcal/mol) are relative to CB_5H_7.

The H_2 complex $CB_9H_9(ax)$ is only 8.7 kcal/mol higher in energy than the H-capped CB_9H_{11} species (Figure 3). The H−H distance in the complex is very short (0.875 Å), yet the H_2 molecule is bound by 20.4 kcal/mol to $CB_9H_9(ax)$. A H_2 complex does not exist when removing the capping hydrogen and one equatorial B−H hydrogen for $CB_9H_9(eq)$. Rather, a transition state (13.3 kcal/mol higher than CB_9H_{11}) is found for forming two equivalent CB_9H_{11} structures. The H−H distance is 0.811 Å, and the transition state is 6.6 kcal/mol below the $CB_9H_9(eq) + H_2$ asymptote.

There is a significant difference in stability between CB_9H_9-(ax) and $CB_9H_9(eq)$. The $CB_9H_9(eq)$ is 9.2 kcal/mol more stable than $CB_9H_9(ax)$. Thus $CB_9H_9(eq)$ can form more readily than $CB_9H_9(eq)$ and can add a fluoride ion to the electron-deficient boron atom, presumably without additional activation barrier to form **B5** from $CB_9H_9(ax) + F^-$ or **B8** from $CB_9H_9(eq) + F^-$.

For $n = 5$ and $n = 11$, $CB_nH_n(ax)$ is more stable than CB_nH_n-(eq) by 4.6 and 4.5 kcal/mol,[20] respectively. In contrast, for $n = 9$, $CB_9H_9(eq)$ is 9.2 kcal/mol more stable than $CB_9H_9(ax)$. The energy preference can be understood when one considers charge distributions. For $n = 5$ and $n = 11$, the cage is based on the regular octahedron and icosahedron, respectively, where positions are identical. For $n = 9$, the square-bicapped antiprism has two different positions in a 2:8 ratio of axial to equatorial. The concept of topological charge stabilization[23] indicates that a B^+ substitution for BH ($CB_nH_n \leftarrow CB_nH_{n+1}^-$) would prefer

(19) Liquid HF has a dielectric constant of 83.6 at 273.2 K. See: *CRC Handbook of Chemistry and Physics*, 80th ed.; CRC Press: Boca Raton, 2000.

(20) Rankin, K. N.; Chandler, W. D.; Johnson, K. E. *Can. J. Chem.* **1999**, *77*, 1599.

(21) Tomita, H.; Luu, H.; Onak, T. *Inorg. Chem.* **1991**, *30*, 812.

(22) (a) Bühl, M. NMR Chemical Shift Computations: Structural Applications. In *Encyclopedia of Computational Chemistry*; Schleyer, P. v. R., Allinger, A., Clark, T., Gasteiger, J., Kollmann, P. A., Schaefer, H. F., Schreiner, P. R., Eds.; Wiley: Chichester, U.K., 1998; pp 1835−1845. (b) Onak, T. In *The Borane, Carborane, Carbocation Continuum*; Casanova, J., Ed.; Wiley: New York, 1998; pp 247−258. (c) Onak, T.; Diaz, M.; Barfield, M. *J. Am. Chem. Soc.* **1995**, *117*, 1403.

(23) Ott, J. J.; Gimarc, B. M. *J. Am. Chem. Soc.* **1986**, *108*, 4303.

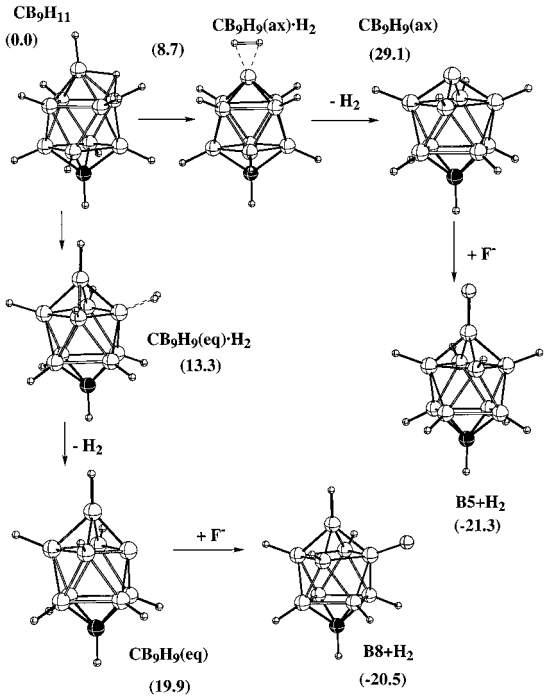

Figure 3. Ionic HF fluorination pathway of $CB_9H_{10}^-$. The complex of H_2 with CB_9H_9(eq) is a transition state (not a minimum). CB_9H_9-(eq) is 9.2 kcal/mol more stable than CB_9H_9(eq). All energies (kcal/mol) are relative to CB_9H_{11}.

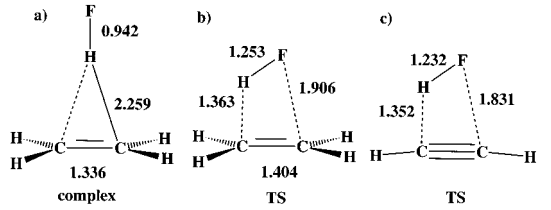

Figure 4. (a) HF−C_2H_4 complex and (b) HF addition transition state to ethylene calculated at the B3LYP/6-31G(d) level.[24] (c) HF addition transition state to acetylene calculated at the QCISD/6-311(2d,2p) level.[25a]

an equatorial position to an axial position since the equatorial positions are more positively charged in the $CB_9H_{10}^-$ anion. In $CB_5H_6^-$ and $CB_{11}H_{12}^-$, where all vertexes have very similar charges, the site preference is not strong.

Concerted HF Fluorination. The transition states for addition of HF to C_2H_4 and C_2H_2 have recently been calculated.[24−26] For the HF + C_2H_4 reaction, an initial complex has been calculated (bound by 3.8 kcal/mol at MP2/6-311G(3df,2p)//B3LYP/6-31G(d) at 0 K) where the hydrogen of HF is bridging the two carbon centers (Figure 4). The bridging structure of the complex is to be expected since the $C_2H_5^+$ cation is known[27] to have a nonclassical structure with a bridging hydrogen. The calculated activation barrier for HF addition is 51.1 kcal/mol with respect to separated reactants. In very recent work, Cremer et al.[26] have used the CCSD(T)/cc-pVTZ//CCSD(T)/cc-pVTZ + ZPC/B3LYP/6-311++G(3df,3pd) level of theory with corrections for BSSE and heat capacity (298 K) to calculate a complexation enthalpy of 2.2 kcal/mol and a barrier of 48.3 kcal/mol (relative to separated reactants). The calculated barrier for HF addition to C_2H_4 is considerably reduced if the HF dimer is the reactant rather than an isolated HF molecule.[28−31] The addition of HF to C_2H_2 has a similar activation barrier to the HF + C_2H_4 reaction (52.2 kcal/mol at QCISD(T)/6-311G-(2d,2p)//QCISD/6-311G(2d,2p)).[25a]

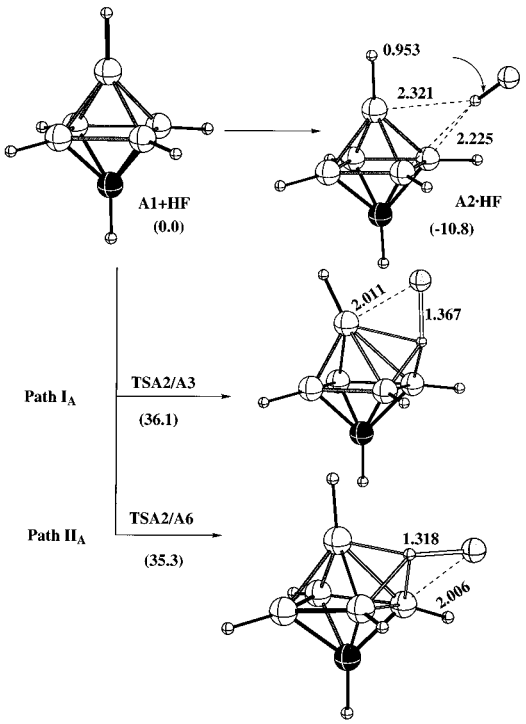

Figure 5. Molecular plots of the initial complex between HF and $CB_5H_6^-$ (**A2**·HF) and the transition states (**TSA2**/**A3** and **TSA2**/**A6**) for addition to the axial and equatorial boron atoms, respectively. The transition state for equatorial addition is 0.8 kcal/mol lower than for axial addition. All energies (kcal/mol) are relative to $CB_5H_6^-$ + HF.

In the concerted HF addition, it is likely that a HF molecule would complex to $CB_5H_6^-$ with the hydrogen end directed toward the center of the BBB face which is known to be protonated in CB_5H_7. In the case that $CB_5H_6^-$ is initially protonated, then the most probable site of attack of the fluoride ion is on the acidic capping hydrogen. In this sense, the ionic and concerted pathways join together if fluoride ion addition to CB_nH_{n+2} is faster than H_2 elimination (see Scheme 1).

The HF is bound by 10.8 kcal/mol in **A2**·HF (Figure 5). For HF addition to $CB_5H_6^-$, the activation barrier (**TSA2**/**A3**) is 36.1 kcal/mol (with respect to separated reactants) for addition to the axial position and 35.3 kcal/mol (**TSA2**/**A6**) for addition to the equatorial position (Figure 5). A *nido* cage (**A3**) is formed from HF addition to the axial position (Figure 6, path I_A) which is 5.3 kcal/mol higher in energy than $CB_5H_6^-$ + HF with an endo fluoride substituent. An endo (**A3**) to exo (**A4**) rearrangement of the fluoride substituent is possible by a 90° rotation of the BHF group to reach the transition state **TSA3**/**A4** ($\Delta H^{\ddagger}$ =

(24) Senger, S.; Radom, L. *J. Phys. Chem. A* **2000**, *104*, 7375.
(25) (a) Martínez-Núñez, E.; Vázquez, S. A. *Chem. Phys. Lett.* **2000**, *332*, 583. (b) For very similar results on the HF + C_2H_2 → CH_2CHF reaction, see: Lin, S.-R.; Lin, S.-C.; Lee, Y.-C.; Chou, Y.-C.; Chen, I.-C.; Lee, Y.-P. *J. Chem. Phys.* **2001**, *114*, 7396.
(26) Cremer, D.; Wu, A.; Kraka, E. *Phys. Chem. Chem. Phys.* **2001**, *3*, 674. Also see this reference for a review of prior theoretical and experimental work.
(27) See: Perera, S. A.; Bartlett, R. J.; Schleyer, P. v. R. *J. Am. Chem. Soc.* **1995**, *117*, 8476.
(28) Menéndez, M. I.; Suárez, D.; Sordo, J. A.; Sordo, T. L. *J. Comput. Chem.* **1995**, *16*, 659.
(29) Menéndez, M. I.; Sordo, J. A.; Sordo, T. L. *THEOCHEM* **1996**, *371*, 91.
(30) Clavero, C.; Duran, M.; Lledós, Ventura, O. N.; Bertrán, J. *J. Am. Chem. Soc.* **1986**, *108*, 923.
(31) Jursic, B. S. *THEOCHEM* **1998**, *434*, 37.

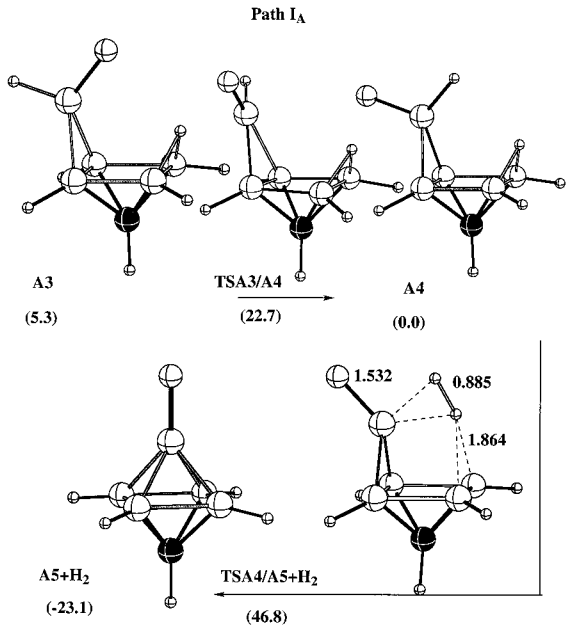

Figure 6. Molecular plots for path I_A (addition to $CB_5H_6^-$ axial boron) including the endo (**A3**) to exo (**A4**) rearrangement and H_2 elimination from **A4** to form **A5**+H_2. All energies (kcal/mol) are relative to $CB_5H_6^-$ + HF.

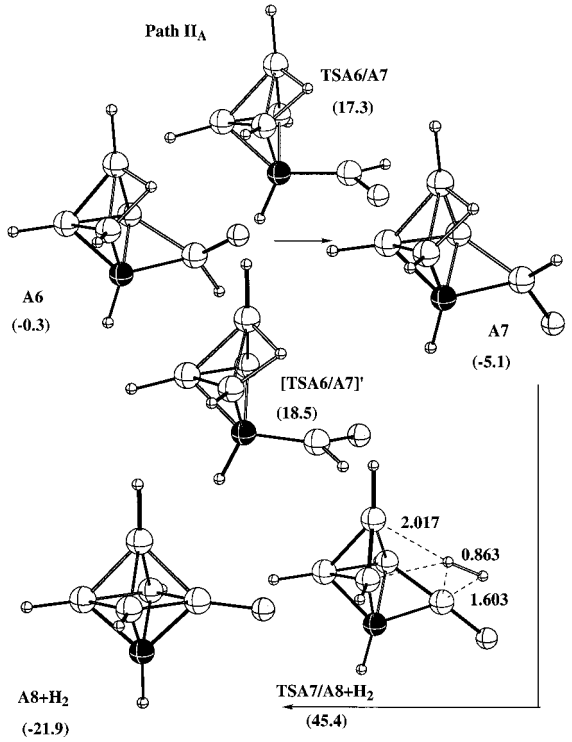

Figure 7. Molecular plots for path II_A (addition to $CB_5H_6^-$ equatorial boron). There are two transition states for the endo (**A6**) to exo (**A7**) rearrangement depending on whether the BHF group rotates toward (**TSA6**/**A7**) or away from ([**TSA6**/**A7**]′) the carbon atom. All energies (kcal/mol) are relative to $CB_5H_6^-$ + HF.

17.4 kcal/mol). The *exo*-F-*nido* cage (**A4**), 5.3 kcal/mol more stable than the *endo*-F-*nido* cage (**A3**), can eliminate molecular H_2 through **TSA4**/**A5**+H_2 with a barrier of 46.8 kcal/mol. The resulting products, *closo*-6-$CB_5H_5F^-$ plus H_2, are 23.1 kcal/mol more stable than reactants $CB_5H_6^-$ + HF.

If HF adds to an equatorial boron atom (Figure 7, path II_A), the *endo*-F-*nido* cage **A6** results which can rearrange to the *exo*-F-*nido* cage **A7** by rotating the BHF group toward the carbon atom (**TSA6**/**A7**, $\Delta H^{\ddagger} = 17.6$ kcal/mol) or away from the carbon atom (**[TSA6**/**A7]′**, $\Delta H^{\ddagger} = 18.9$ kcal/mol). From **A7**, molecular hydrogen can be eliminated through **TSA7**/**A8**+H_2 ($\Delta H^{\ddagger} = 50.5$ kcal/mol) to reach *closo*-2-$CB_5H_5F^-$ plus H_2, which are 21.9 kcal/mol more stable than reactants $CB_5H_6^-$ + HF.

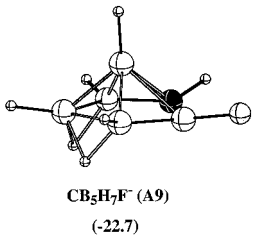

Figure 8. Molecular plot of **A9**, the global minimum on the $CB_5H_7F^-$ potential energy surface.

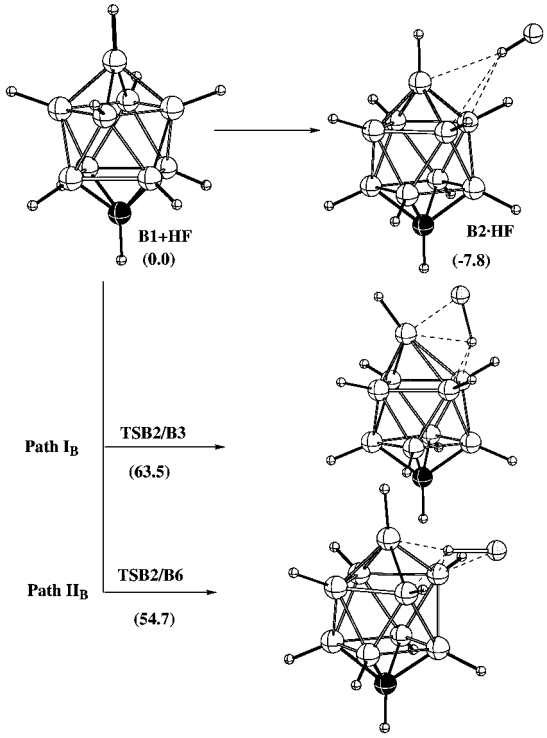

Figure 9. Molecular plots of the initial complex between HF and $CB_9H_{10}^-$ (**B2**·HF) and the transition states (**TSB2**/**B3** and **TSB2**/**B6**) for addition to the axial and equatorial boron atoms, respectively. The transition state for equatorial addition is 8.8 kcal/mol lower than for axial addition. All energies (kcal/mol) are relative to $CB_9H_{10}^-$ + HF.

It is known that fluoride ion plus 1,6-*closo*-$C_2B_4H_6$ gives 5-F-*nido*-2,4-$C_2B_4H_6^-$ as the only detectable product. It is interesting to know whether a corresponding structure exists in the reaction of HF with $CB_5H_6^-$. In fact, the corresponding *nido* compound **A9** was located (Figure 8) and found to be the global minimum, 22.7 kcal/mol more stable than reactants. A corresponding structure is less likely on the HF + $CB_9H_{10}^-$ surface due to the constraints imposed by the lower belt of four boron atoms. Thus, while $CB_5H_6^-$ may provide a model for pathways on the $CB_9H_{10}^-$ potential energy surface, the actual reaction in the model system may be affected by the presence of the stable *nido* cage **A9** on the potential energy surface.

Turning from the model to the actual system (Figure 9), the HF complex with $CB_9H_{10}^-$ (**B2**·HF) is very similar to the **A2**· HF complex in that the hydrogen of HF is capping the same BBB face. The HF binding energy in **B2**·HF (7.8 kcal/mol) is slightly smaller than in **A2**·HF (10.8 kcal/mol). There is a much

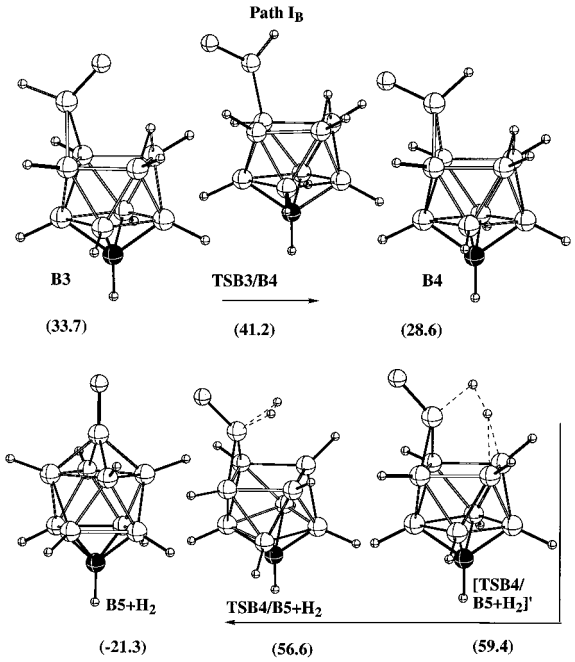

Figure 10. Molecular plots for path I_B (addition to $CB_9H_{10}^-$ axial boron) including the endo (**B3**) to exo (**B4**) rearrangement and H_2 elimination from **B4** to form **B5**+H_2. The stationary point [**TSB4**/**B5**+H_2]′ has two imaginary frequencies. All energies (kcal/mol) are relative to $CB_9H_{10}^-$ + HF.

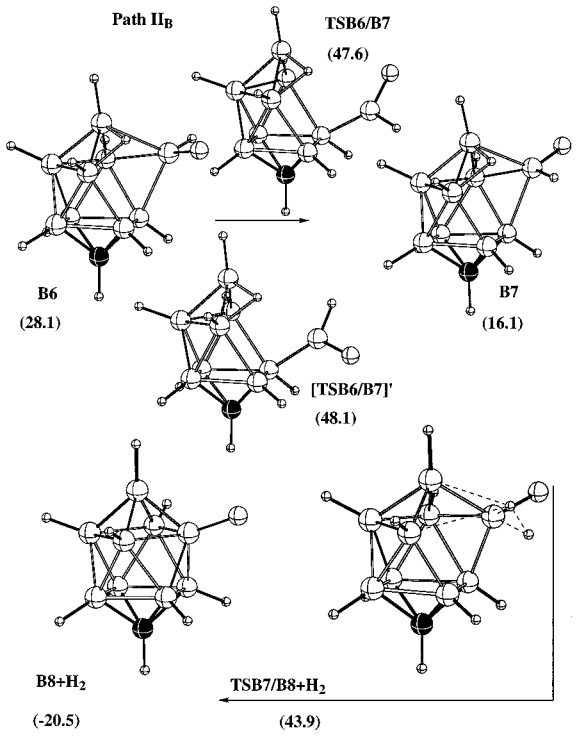

Figure 11. Molecular plots for path II_B (addition to $CB_9H_{10}^-$ equatorial boron). There are two transition states for the endo (**B6**) to exo (**B7**) rearrangement depending on whether the BHF group rotates away from (**TSB6**/**B7**) or toward ([**TSB6**/**B7**]′) the carbon atom. All energies (kcal/mol) are relative to $CB_9H_{10}^-$ + HF.

larger difference between the enthalpies of the two transition states for addition of HF to the axial boron (**TSB2**/**B3**, $\Delta H^{\ddagger} =$ 71.3 kcal/mol) and the equatorial boron (**TSB2**/**B6**, $\Delta H^{\ddagger} = 62.5$ kcal/mol). While it is likely that the barrier height would be substantially reduced in LAHF, the 8.8 kcal/mol energy between **TSB2**/**B3** and **TSB2**/**B6** can easily rationalize the absence of substitution at the axial position.

The *endo*-F-*nido* cage from axial HF addition (Figure 10, path I_B, **B3**) is very similar to **A3**. The rotation of the BHF group from endo to exo goes through a transition state (**TSB3**/**B4**, $\Delta H^{\ddagger} = 7.5$ kcal/mol) where the BHF group is covalently bonded to one boron rather than bridging as in **TSA3**/**A4**. From **B4**, a stationary point (**[TSB4**/**B5**+H_2**]**′) with two imaginary frequencies was located for elimination of molecular H_2 which is 30.8 kcal/mol above **B4**. A true transition state (**TSB4**/**B5**+H_2) was located 2.8 kcal/mol lower in energy where the H_2 moiety is twisted by 90°. While the product obtained from **TSB4**/**B5**+H_2 is **B5** + H_2, from an inspection of the imaginary mode, it is clear that one or more intermediates exist between **TSB4**/**B5**+H_2 and **B4** involving the migration of the bridging hydrogen. The intervening transitions state(s) and intermediate-(s) were not located, but they are believed to be lower in energy than **TSB4**/**B5**+H_2.

Addition of HF to the equatorial boron of $CB_9H_{10}^-$ (Figure 11, path II_B) gives the *endo*-F-*nido* cage **B6** which has two pathways for rearranging to the more stable *exo*-F-*nido* cage (**B7**). The lower-energy pathway (**TSB6**/**B7**, $\Delta H^{\ddagger} = 19.5$ kcal/mol) involves breaking two B−B interactions and a substantial rotation around the B−B covalent bond. The *exo*-F-*nido* product **B7** is obtained by re-forming the two B−B interactions. The alternative pathway through [**TSB6**/**B7**]′ (0.5 kcal/mol higher than **TSB6**/**B7**) involves initial breaking of two B−B interactions to form the transition state and then substantial rotation about the B−B covalent bond to form the **B7** product. From **B7**, the transition state for elimination of molecular hydrogen (**TSB7**/**B8**+H_2) is reached with a barrier of 27.8 kcal/mol to form **B8** + H_2.

Thus the fluorinated *closo* cage 10-$CB_9H_9F^-$ (**B5**) is the thermodynamic product (0.8 kcal/mol more stable than **B8**), while the observed product is the 6-$CB_9H_9F^-$ isomer (**B8**). If the reaction follows the ionic HF fluorination pathway, then the reaction is controlled by the formation of CB_9H_9(eq) which is 9.2 kcal/mol more stable than CB_9H_9(ax). If the reaction follows the covalent HF fluorination pathway, then the reaction is controlled by the initial activation barrier for addition of HF which is 8.8 kcal/mol higher to form the fluorinated cage which leads to 10-$CB_9H_9F^-$ compared to the cage which leads to the 6-$CB_9H_9F^-$ product. If the $CB_9H_{10}^-$ cage is initially protonated followed by F^- addition, the initial cage formed may be the more stable *exo*-F-*nido* complex **A4** or **B4**, thus bypassing the *endo*-F-*nido* complexes **A3** or **B3** which would be formed in the concerted HF fluorination pathway. In fluorination of *closo*-1,6-$C_2B_4H_6$ by F^-, the initial product formed is an *exo*-F-*nido* cage.[32]

It is known that a second HF molecule can substantially reduce the calculated activation barrier for the addition of HF to C_2H_4.[28−31] Therefore, it was of interest to determine the effect of a second HF molecule on the fluorination of $CB_5H_6^-$ (**A1**). The two HF molecules are bound by 21.4 kcal/mol in the initial complex (Figure 12, **A2**·2HF). From **A2**·2HF two stationary points were located,[33] one for the addition of fluorine to the axial boron (**TSA2**·2HF/**A3**+HF) and one for the addition of fluorine to an equatorial boron **(TSA2**·2HF/**A6**+HF). With the second HF, equatorial addition is still favored over axial addition

(32) McKee, M. L. Work in progress.

(33) Both structures, **TSA2**·2HF/**A3**+HF and **TSA2**·2HF/**A6**+HF, are characterized by second small imaginary frequencies (16i and 26i cm^{-1}, respectively). When the C_s symmetry constraint was relaxed in **TSA2**·2HF/**A3**+HF, a transition state to **A1**−H^++FHF^- was obtained.

Table 3. Reaction Enthalpies and Activation Barrier for the Fluorination Reaction of $CB_nH_{n+1}^-$ at the Axial and Equatorial Positions

	$n = 5$ (**A1**, $CB_5H_6^-$)		$n = 9$ (**B1**, $CB_9H_{10}^-$)	
	axial	equatorial	axial	equatorial
Ionic HF Fluorination				
$CB_nH_{n+1}^- + (HF)_2 \rightarrow CB_nH_{n+2} + FHF^-$	10.4		37.0	
$\rightarrow CB_nH_n + H_2 + FHF^-$ (barrier)	58.5	63.1	66.1	56.9
$\rightarrow CB_nH_nF^- + H_2 + HF$	−22.4	−21.2	−20.6	−19.8
Covalent HF Fluorination				
$CB_nH_{n+1}^- + (HF)_2 \rightarrow CB_nH_{n+1}^-\cdot HF + HF$	−10.1		−7.1	
$\rightarrow CB_nH_{n+2}F^- + HF$ (barrier)	36.8	36.0	64.2	55.4
$\rightarrow CB_nH_nF^- + H_2 + HF$	−22.4	−21.2	−20.6	−19.8

by 2.2 kcal/mol, which is slightly more than the difference found when the reactant is a single HF molecule. The second HF molecule shows a strong catalytic effect, lowering the activation barrier 15.4 kcal/mol for axial addition (46.9 versus 31.5 kcal/mol) and 16.8 kcal/mol for equatorial addition (46.1 versus 29.3 kcal/mol). It is interesting to point out that the second HF molecule provides stabilization but is not involved in a proton relay such as that calculated in the reaction between $(HF)_2$ and C_2H_4.[28,30]

The transition state with the lowest activation barrier (23.5 kcal/mol) was for proton transfer to give **A1**−H^+ plus FHF^- (**TSA2**·2HF/**A1**−H^++FHF^-). While the isolated products (**A1**−H^+ and FHF^-) are 6.8 kcal/mol *higher* in energy than the transition state, the binding energy of the product complex should make the reaction exothermic. It is anticipated that larger clusters of HF $(HF)_n$, $n > 2$, would further reduce the activation barrier.

A summary of the reaction energies and activation barriers is given in Table 3 where the fluorination agent is taken to be the HF dimer. Since the effect of solvation in LAHF is expected to be large, the calculations cannot predict which pathway will be favored. However, equatorial is favored over axial fluorination in all cases except ionic fluorination of $CB_5H_6^-$. For $CB_9H_{10}^-$, equatorial is favored over axial by 9.2 kcal/mol for ionic HF fluorination and by 8.8 kcal/mol for covalent HF fluorination.

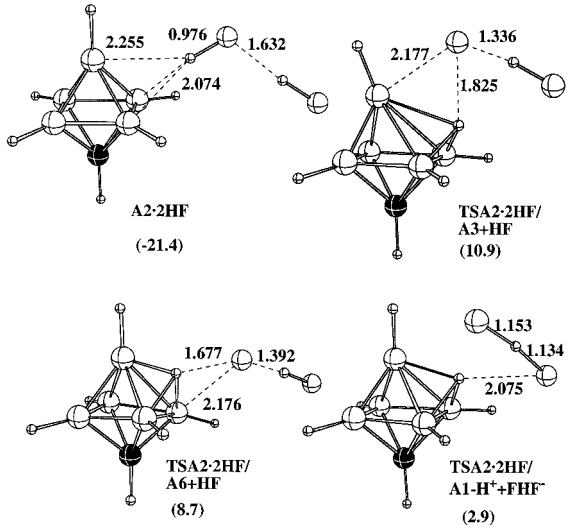

Figure 12. Molecular plots of the complex between two HF molecules and $CB_5H_6^-$ (**A2**·2HF), the stationary structures for axial addition (**TSA2**·2HF/**A3**+HF) and equatorial addition (**TSA2**·2HF/**A6**+HF) of molecular HF to $CB_5H_6^-$, and the transition state for proton transfer from the comlex to form CB_5H_7 plus FHF^- (**TSA2**·2HF/**A1**−H^++FHF^-). All energies (kcal/mol) are relative to $CB_5H_6^- + 2HF$.

Conclusions

The fluorination of $CB_5H_6^-$ and $CB_9H_{10}^-$ by HF was studied by considering two pathways: ionic HF fluorination where the cage is first protonated, followed by H_2 elimination and then F^- addition; and covalent HF fluorination where HF adds concertedly to the cage, followed by an internal endo to exo rearrangement, and then H_2 elimination. The pathways are probably comparable in energy in LAHF and lead to the same conclusion that fluorination should take place at an equatorial position in $CB_9H_{10}^-$ which is consistent with experimental observations. It would be interesting to conduct experiments on $CB_9H_{10}^-$ in LAHF to determine which pathway (ionic or covalent) is operative.

Acknowledgment. Computer time was provided by the Alabama Supercomputer Network and Maui High Performance Computer Center. M.L.M. would like to thank Sun Microsystems Computer Corporation for the award of an Academic Equipment Grant.

Supporting Information Available: Cartesian coordinates for relevant structures optimized at the B3LYP/6-31G(d) level. This material is available free of charge via the Internet at http://pubs.acs.org.

IC010176H